Supplement of The Cryosphere, 19, 2751–2768, 2025
https://doi.org/10.5194/tc-19-2751-2025-supplement

The Cryosphere Open Access EGU

Supplement of

Impact of modulating surface heat flux through sea ice leads on Arctic sea ice in EC-Earth3 in different climates

Tian Tian et al.

Correspondence to: Tian Tian (tian@dmi.dk)

Below are Supplementary Figures S1-S6

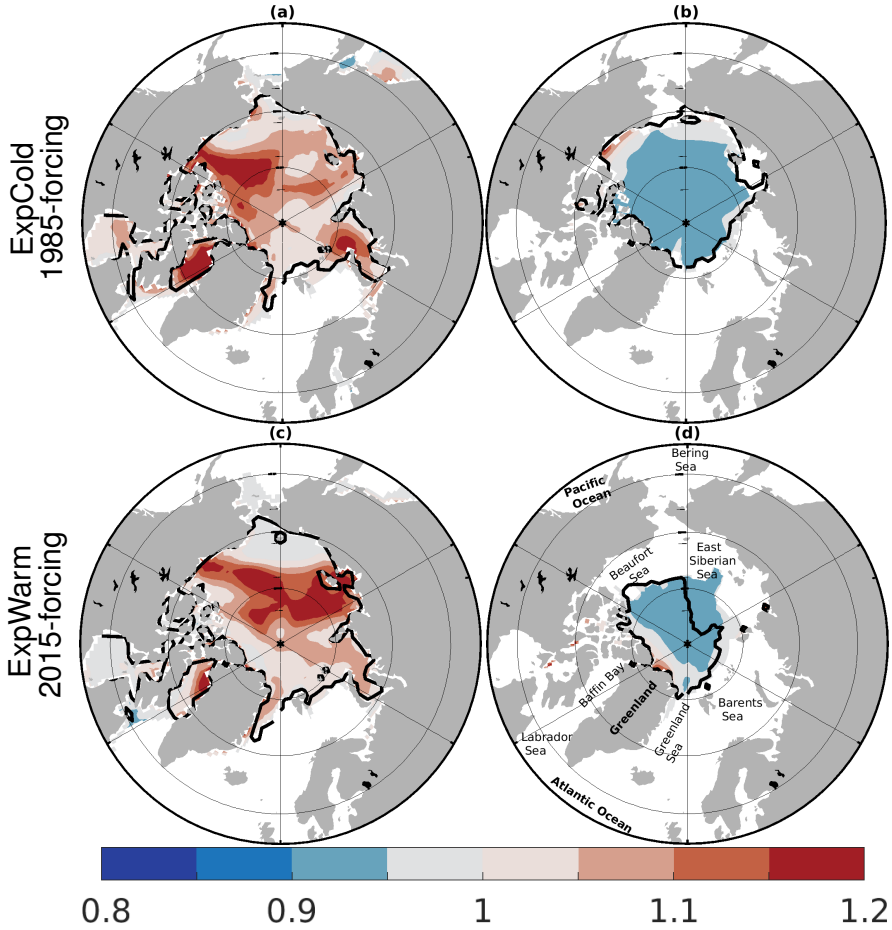

Figure S1. Factor modulating the turbulent heat fluxes over Arctic sea ice (SIC>70 %): (a) Late winter and (b) later summer for ExpCold. (c) and (d) as (a) and (b), but for ExpWarm. The regions with sea ice thickness $>$ 1 m in the PIOMAS reanalysis are compassed by black thick lines. Note: color only for the regions with SIC>70 %, while white areas indicating a constant factor of 1 (i.e. SIC $\leq$ 70 %).

The figure illustrates the modulation of turbulent heat fluxes over sea ice, showing remarkable seasonal variation and such effect in different magnitudes between ExpCold and ExpWarm scenarios, particularly in regions with sea ice thicker than 1 m.

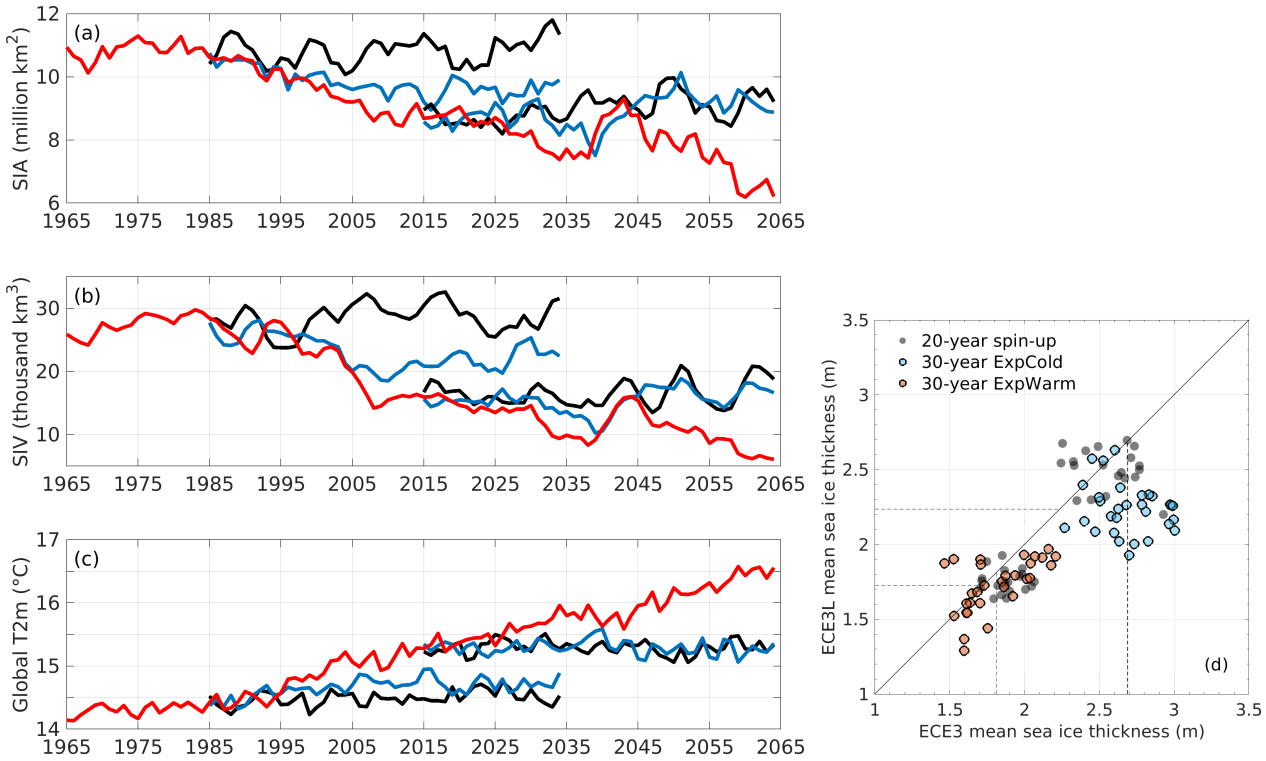

Figure S2. Yearly mean time series of Arctic sea ice area (a), Arctic sea ice volume (b) and global 2-meter air temperature (c) from 1965 to 2065. Comparisons are shown across three simulations: the ECE3 (black), ECE3L (blue), and a transient (r5) simulation, driven by historical and SSP2-4.5 external forcings (red). Results from the 1985-forcing experiments are shown for the period 1985–2034, while results from the 2015-forcing experiments cover the period 2015–2064. d) Scatter plot comparing the 30-year mean sea ice thickness (SIV/SIA, in meters) between ECE3 and ECE3L simulations. The diagonal line represents a 1:1 ratio, where points above indicate thicker ice in ECE3L and points below indicate thinner ice. Colors differentiate between the 30-year ExpCold (blue) and ExpWarm (red) periods, while the 20-year spin-up phase is shown in gray. Dashed lines indicate 30-year means for each dataset.

The changes in sea ice area and volume from ECE3 to ECE3L shows notable differences between the ExpCold and ExpWarm setups, revealing the sensitivity of sea ice evolution to initial sea ice conditions and external forcing, with relatively more sea ice reduction in ExpCold. The paired simulations are stable over the 50 year period in both forcing experiments, with no significant warming trends attributable to initialization artifacts. This stability is reflected in the absence of noticeable temperature drift in both forcing periods. In contrast, the transient simulation (r5), driven by historical and SSP2-4.5 external forcings, shows a clear warming trend over time. The small fluctuations in ECE3 and ECE3L are consistent with internal variability, indicating that the model does not exhibit any pronounced initialization-induced warming.

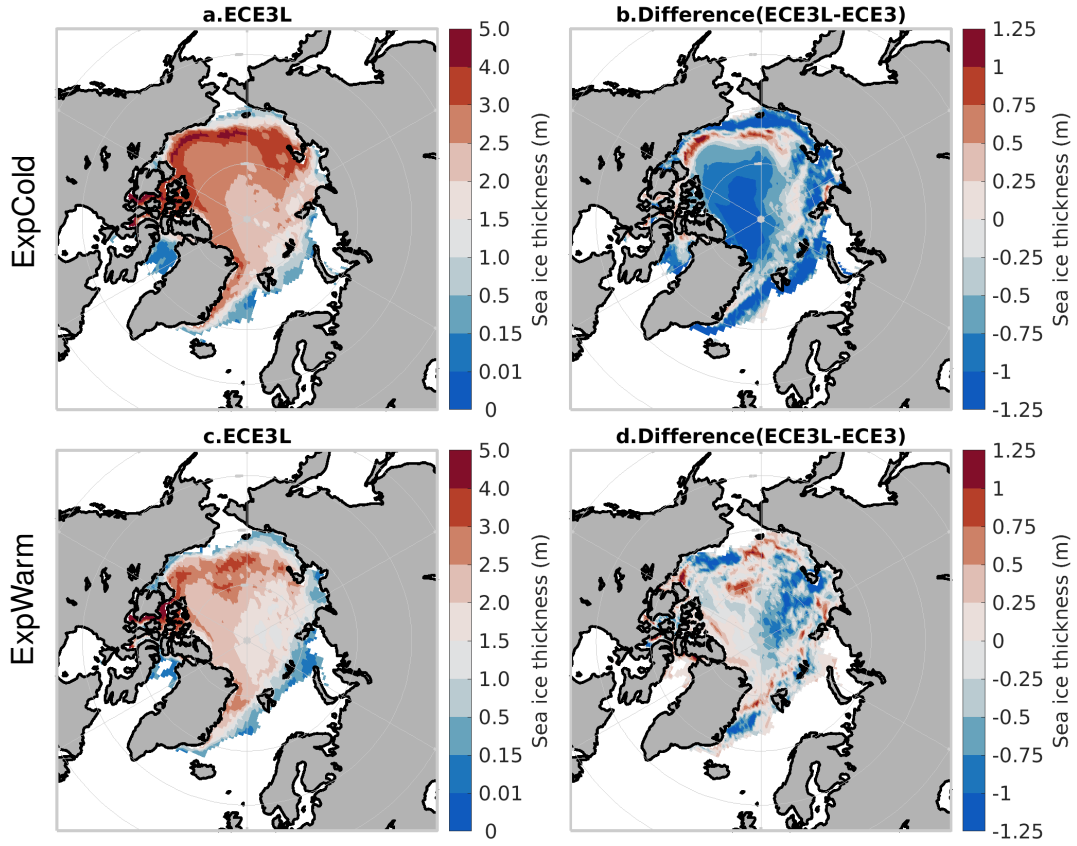

Figure S3. The late-summer (September) Arctic sea ice thickness under a constant forcing for ExpCold (a) ECE3L and (b) the ECE3L minus ECE3 differences. Panels (c) and (d) are the same as panels (a) and (b) but for ExpWarm. Values are shown as 30 year averages, as in Fig. 2. Note that a nonlinear colour scale is used to emphasize low ice thicknesses. Thicknesses under 0.01 m are not shown.

In summer the regions experiencing the greatest SIT reduction remain consistent with those identified in winter, as shown in Fig. 3: from the eastern Arctic in the thicker ice regions in ExpCold shifting to the western Arctic in the thinner ice regions in ExpWarm.

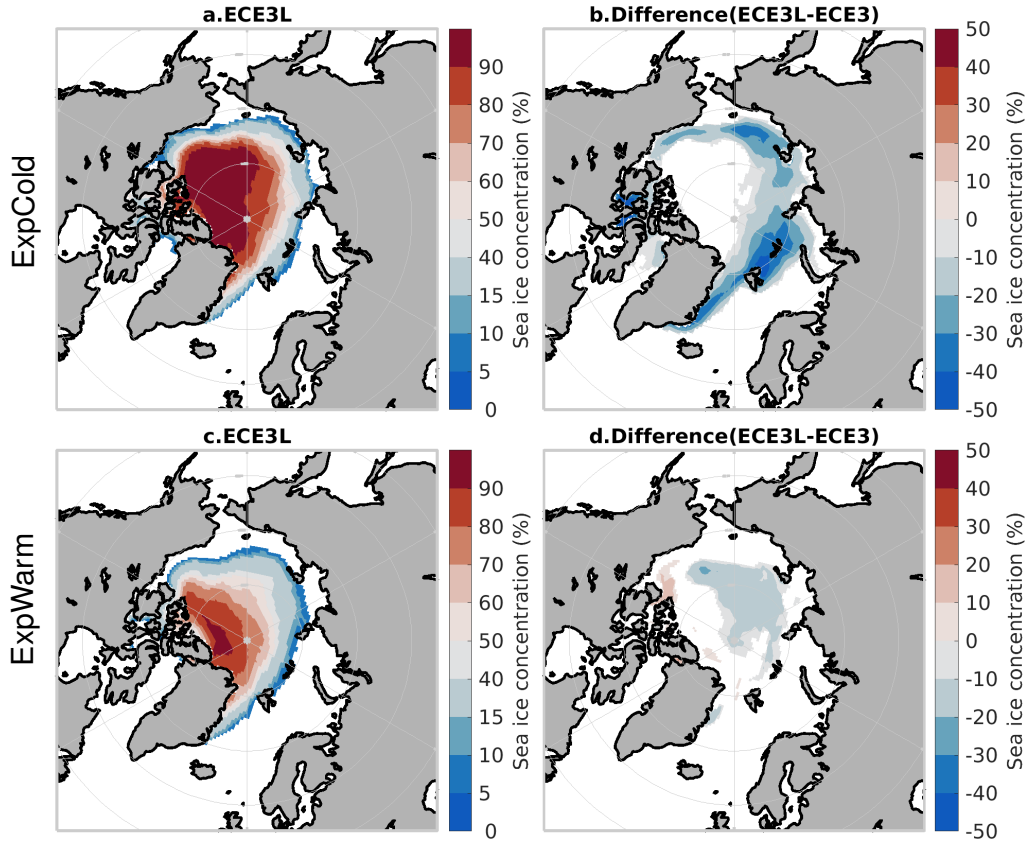

Figure S4. The late-summer (September) Arctic sea ice concentration under a constant forcing for ExpCold (a) ECE3L and (b) the ECE3L minus ECE3 differences. Panels (c) and (d) are the same as panels (a) and (b) but for ExpWarm. Values are shown as 30 year averages, as in Fig. 2. Note that a nonlinear colour scale is used to emphasize low ice concentrations. Concentrations under 5 % are not shown.

In summer the regions experiencing the greatest SIC reduction remain consistent with those identified in winter, as shown in Fig. 4. These are primarily in the thinner ice regions, typically along the ice margins, with up to 30% reduction in ExpCold compared to less than 20% in ExpWarm.

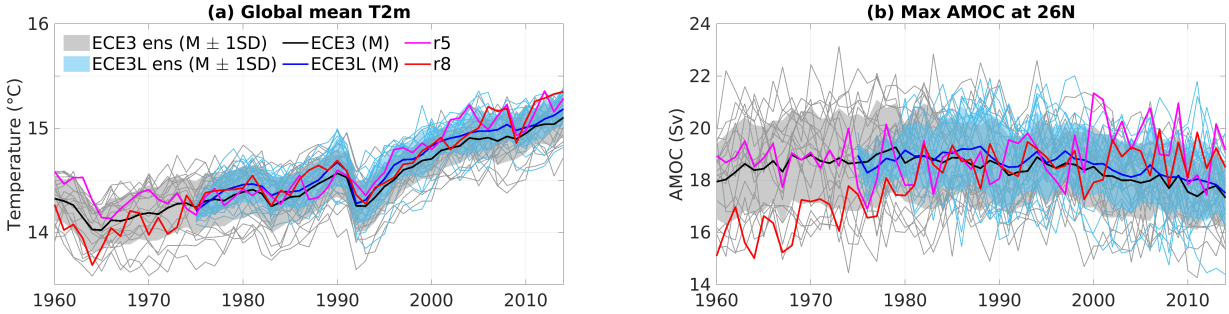

Figure S5. Time series of annual mean global T2m and the Atlantic Meridional Overturning Circulation (AMOC), measured as the maximum of the stream function below 500 m at 26°N in the historical simulations. The ECE3 and ECE3L members (thin lines) are indicated with ensemble means (thick line) and model spread (shaded area) represented as one standard deviation from the ensemble mean across 20 members. Note r5 and r8 are indicated by pink and red lines.

For the generation of the ECE3L ensemble, we introduced small random perturbations (on the order of 10^{-5} °C) in the 3D temperature field. Although these perturbations are minor, they are adequate to induce divergence among ensemble members after only a few days. We compared the ensemble mean and the model spread for TAS (a), and AMOC (b) between ECE3L and the original ECE3 ensemble. We applied paired t-test to assess statistical differences over the period from 1980 to 2014. Although the difference in AMOC between r5 and r8 has converged since 1980, the ECE3L simulations exhibit a model spread (std=1.4 Sv) similar to that of ECE3 (std=1.5 Sv), with an ensemble mean difference of -0.3 Sv (ECE3 - ECE3L). This difference is statistically significant ($p < 0.05$), indicating that our method captures the internal variability of AMOC adequately. Similar to the global mean T2m, both simulations exhibit a comparable model spread of 0.2 °C, with an ensemble mean difference of -0.1 °C. This difference between the ensemble mean time series is statistically significant ($p < 0.05$). However, the detrended time series do not show a significant difference ($p > 0.05$), suggesting that external forcing plays a dominant role in the observed variations.

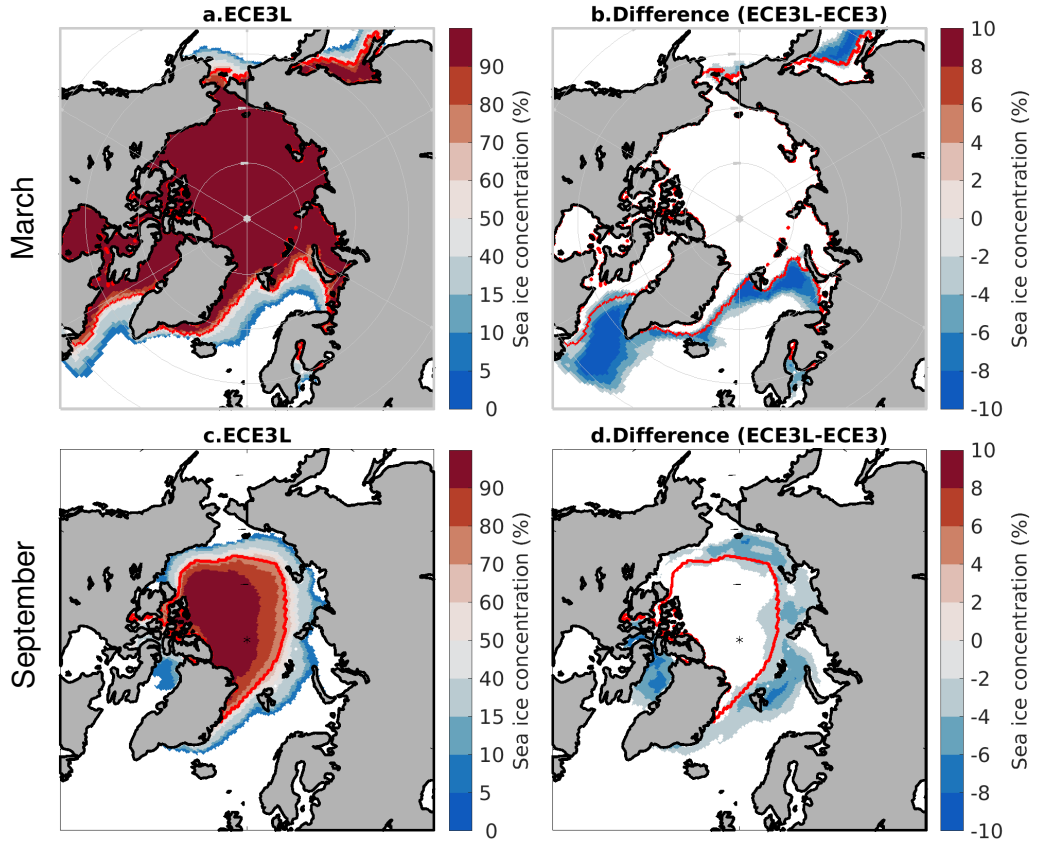

Figure S6. Ensemble mean Arctic maps (1980–2014) for the (a) ECE3L March sea ice concentration and (b) ECEL minus ECE3 difference. Panels (c) and (d) are the same as panels (a) and (b) but for September. Note that a nonlinear colour scale is used to emphasize low ice concentrations. Concentrations under 5 % are not shown. The areas with SIC$\geq$70% in both ECE3 and ECE3L are compassed by red lines.

The regions showing the greatest SIC reduction in March and September climatologies are similar to those observed in ExpCold (Figs. 4a,b and S4a,b), though the magnitude of the reduction is lower compared to ExpCold.